SUPPLEMENTAL FIGURES AND TABLES

Table S1. Strains and plasmids used in this study.

Strain/plasmid	***Characteristics***	***Source/reference***
Strain		
E. coli		
TOP10	F$^-$ *mcrA Δ(mrr-hsdRMS-mcrBC) ∅80lacZΔM15 lacX74 recA1 deoR araD139 Δ(ara-leu)7697 galU galK rpsL (Str^r) endA1*	Invitrogen
TG1	*supE hsd D5 thi Δ(lac-proAB)* F'*(traD36 proAB-lacZ ΔM15)*	(71)
BL21 (DE3)	*lacI^q rrnB$_{T14}$ ΔlacZ$_{WJ16}$ hsdR514 ΔaraBA-D$_{AH33}$ ΔrhaBAD$_{LD78}$*	Invitrogen
K-12 BW25113	*lacI^q rrnB$_{T14}$ ΔlacZ$_{WJ16}$ hsdR514 ΔaraBAD$_{AH33}$ ΔrhaBAD$_{LD78}$*	(72)
K-12 BW25113 *ahpC*		(72) http://ecoli.naist.jp/
L. lactis		
MG1363	WT strain referred as WT strain.	(73)
S. agalactiae		
NEM316	Serotype III isolated from neonatal blood culture	(74)
NEM2175	NEM316 *ahpC*::*aphA-3*. Km^R	This study
Plasmid		
pG+host5	Temperature-sensitive vector. Em^R	(31)
pET100/D-TOPO	Cloning vector. Ap^R	Invitrogen
pHis-AhpC	Expression of N-terminal His-tagged AhpC. Cloned into pET100/D-TOPO.	This study
pHis-AhpC$^{C47A, C164A}$	Expression of N-terminal His-tagged AhpC$^{C47A\ C164A}$. Cloned into pET100/D-TOPO.	This study
pCR-BLUNT	Cloning vector. Km^R	Invitrogen
pMAL-c4X	Cloning vector. Ap^R	New England BioLabs
pMAL-AhpC	Expression of N-terminal MBP-AhpC. Cloned into pMAL-c4X.	This study
pHA-AhpC	Expression of N-terminal HA-tagged AhpC. Native promoter. Cloned into pCR-BLUNT. Km^R	This study
pAhpCF	Expression AhpC and AhpF operon. Native promoter. Cloned into pCR-BLUNT. Km^R	This study
pLUMB5	P$_{aphA-3}$-*katA*-His$_6$. Expression *E. faecalis* KatA. Kanamycin resistance promoter. Cm^R	(42)

Table S2. Oligonucleotides used in this study.

Primer	Sequence 5'-3'	Target
O1	GGAGAATTCATCACTGTTACAAATGAAGACGT	*ahpC*
O2	AAGGGGTACCAATGGGGCATGGATTCACATC	*ahpC*
O3	GGGGTACCTTTAAATACTGTAG	*aphA-3*
O4	TCTGGATCCTAAAACAATTCATCC	*aphA-3*
O5	TTCAGGGGATCCAATGGGGGCATGGATTCACATC	*ahpF*
O6	GTTACCTGCAGGACCACCACCAATAAC	*ahpF*
O7	CACCATGTCATTAGTCGGAAAAGAAATT'	*His-AhpC*
O8	TTAAATTTTACCTACAAGGTCTAA	*His-AhpC*
O9	GACTTTTCATTTGTTGCTCCAACTGAACTTGGT	*C47A*
O10	ACCAAGTTCAGTTGGAGCAACAAATGAAAAGTC	*C47A*
O11	CATCCAGGTGAAGTTGCTCCAGCTAAATGGAAA	*C164A*
O12	TTTCCATTTAGCTGGAGCAACTTCACCTGGATG	*C164A*
O13	*CCAGATTATGCT*GATATCATGTCATTAGTCGGAAAAGAAATT	*HA*-AhpC*
O14	*ATGTATCCATATGATGTTCCAGATTATGCT*GATATC	*HA**
O15	*AACATCATATGGATACAT*AATAATGTCCTCCTTTATTTTTTAATAGCC	*HA*-AhpC*
O16	GCGTGGCATATCTTCGATACCACCCAAGAA	*HA*-AhpC*
O17	GATATC*AGCATAATCTGGAACATCATATGGATACAT*	*HA**
O18	TTATTGTCTGATTAAATAATCAAATGCGCC	*AhpCF*
O19	CAGCTCAAGCTTATCACGATGGA	*AhpCF mutant*
O20	CTTTACGGGCGGCATAAATTGCAG	*AhpCF mutant*
O21	AATTAAGAATTCATGTCATTAGTCGGAAAA	*MBP-AhpC*
O22	AATTAATCTAGATTAAATTTTACCTACAAG	*MBP-AhpC*

The restriction sites included in oligonucleotides are underlined. * HA sequence corresponds to the peptide MYPYDVPDYA.

Table S3. Cumene hydroperoxide sensitivity of GBS WT and *ahpC* strains.

Equivalent dilutions of overnight WT and *ahpC* GBS cultures were plated in top agar on solid medium. Disks impregnated with 3 % cumene hydroperoxide were placed on each plate. When indicated, precultures were supplemented with 1 μM hemin. Growth inhibition rings diameters were measured after 24 h at 37 °C. Results are means ± S.D.

GBS	**Growth inhibition (mm)**	
	no hemin	**+ hemin**
WT	36.3 ± 0.1 (n = 4)	36.3 ± 0.2 (n = 3)
ahpC	43.3 ± 0.1 (n = 4)	43.2 ± 0.1 (n = 3)

Table S4. Effect of hemin on GBS AhpC activity in *E. coli*.

A plasmid overexpressing the GBS *ahpCF* operon was established in the *E. coli* K12 *ahpC* strain (BW25113). Equivalent dilutions of overnight cultures of each strain were plated, and disks impregnated with 3 % cumene hydroperoxide were placed on each plate. When indicated, precultures and solid media were supplemented with 1 mM 5-aminolevulinate (ALA). Growth inhibition ring diameters were measured after 24 h at 37 °C. Results are means ± S.D.; number of experiments are in parentheses.

***E. coli* BW25113**	**Growth inhibition (mm)**	
	-ALA	**+ALA**
WT	19 ± 2 (n = 3)	19 ± 1 (n = 2)
ahpC	32 ± 3 (n = 3)	31 ± 1 (n = 2)
ahpC/AhpCF	14 ± 2 (n = 3)	14 ± 1 (n = 2)

Figure S1. **Properties of a hemin resin-bound protein, AhpC.** (A) Schematic representation of the NEM316 *ahpCF* operon and mutant construction. The *ahpC* (GBS1874) ORF codes for the 21 kDa alkyl hydroperoxide reductase small subunit C and *ahpF* (GBS1875) for the 55 kDa F subunit, a NADH dehydrogenase. The direction of transcription of relevant genes and the positions of putative termination loop (hairpin symbols) were from the genome nucleotide sequence ((72); http:/genolist.pasteur.fr/SagaList/). The insertion position of the kanamycin resistance (*aphA-3*) cassette is shown. The deleted region is delimited by dotted lines. The position of the primers used for mutant construction (O1 to O6) and to clone *ahpC* (O7 and O8) into the pET200/D-TOPO expression vector are marked by black horizontal arrowheads. (B) Verification of the *aphA-3* kanamycin resistance cassette insertion in the GBS *ahpCF* operon. PCR amplification of DNA corresponding to the *aphA-3* insertion was performed with the O19 and O20 oligonucleotides using WT and *ahpC* mutant strain genomic DNA as templates. The PCR products were deposited on agarose gels intact, or for the *ahpC* mutant, after digestion with enzymes uniquely present in the *aphA-3* inserted DNA, as indicated. Oligonucleotides used above are described in Table S2. (C) Amino-acid sequence alignment of the GBS NEM316 AhpC protein with *L. lactis* MG1363 strains (71 % identity)**,** and with the rat hemin-binding protein 23 (HBP23) (38 % identity). Regions of identity are in gray. Boxed residues represent the catalytic domains centered on cysteine residues. Note that AhpC is generally highly conserved among prokaryotes (data not shown).

Figure S2. Purification, heme-binding titration and characterization of the his-AhpC-hemin complex. (A) 6XHis-AhpC and 6XHis-AhpC$^{C47A,\ C165A}$ were purified by nickel-nitrotriacetic acid metal-affinity chromatography. L, cell lysate; P, purified protein. (B) Reduction and oxidation of the AhpC-hemin complex. 10 µM AhpC-hemin complex was reduced with 1 mM dithionite. Reduction of the complex resulted in a shift of the Soret band from 414 nm to 426 nm, suggesting that AhpC is bound to ferric hemin in our experimental conditions. This result was further confirmed by treating the complex with 10 mM of the oxidant ammonium persulfate, which did not modify the absorption value of the Soret band. (C) Spectral changes were recorded between 350 and 600 nm after addition of increments of 0.5 µM or 1 µM hemin to 6 µM His-AhpC. The arrow indicates the increase of A_{414} as a function of increasing amounts of hemin. Background subtracted absorbances at 414 nm were plotted against the hemin concentration (inset). (D) Heme content of the AhpC-hemin complex. The pyridine hemochrome assay was performed on the AhpC-hemin complex. The amount of heme bound to AhpC was calculated by following the absorbance change at 556 nm using a difference extinction coefficient of 28.32 $mM^{-1}.cm^{-1}$ (40).

Figure S3. Purification of MBP-AhpC. MBP-AhpC was purified on amylose resin. L, cell lysate, P, purified protein.

Figure S4. Growth behavior of the *ahpC* mutant. (A) Hemin toxicity is unaffected by *ahpC* inactivation. GBS WT and *ahpC* strains were grown overnight with the indicated concentration of hemin in static conditions. Similar results were obtained in aerated cultures (not shown; note that GBS cannot activate respiration metabolism in

these conditions as it also requires menaquinone). (B) Growth curves of WT and *ahpC* GBS in aerobic fermentation and respiration-permissive conditions. Bacteria were grown as described in Figure 5 legend. The presented results are representative of 3 independent experiments.

REFERENCES

71. Baer, R., Bankier, A.T., Biggin, M.D., Deininger P.L., Farrell, P.J., Gibson, T.J., Hatfull, G., Hudson, G.S., Satchwell S.C., Séguin. C., Tuffnell, P.S. and Barrell, B.G. (1984) Nature **310**, 207-211
72. Baba, T., Ara, T., Hasegawa, M., Takai, Y., Okumura, Y., Baba, M., Datsenko, K. A., Tomita, M., Wanner, B. L., and Mori, H. (2006) *Mol. Syst. Biol*.**2**, 2006.0008
73. Gasson, M. (1983) *J. Bacteriol.* **154**, 1-9
74. Glaser, P., Rusniok, C., Buchrieser, C., Chevalier, F., Frangeul, L., Msadek, T., Zouine, M., Couve, L., Lalioui, L., Poyart, C., Trieu-Cuot, P., and Kunst, F. (2002) *Mol. Microbiol.* **45**, 1499-1513

A

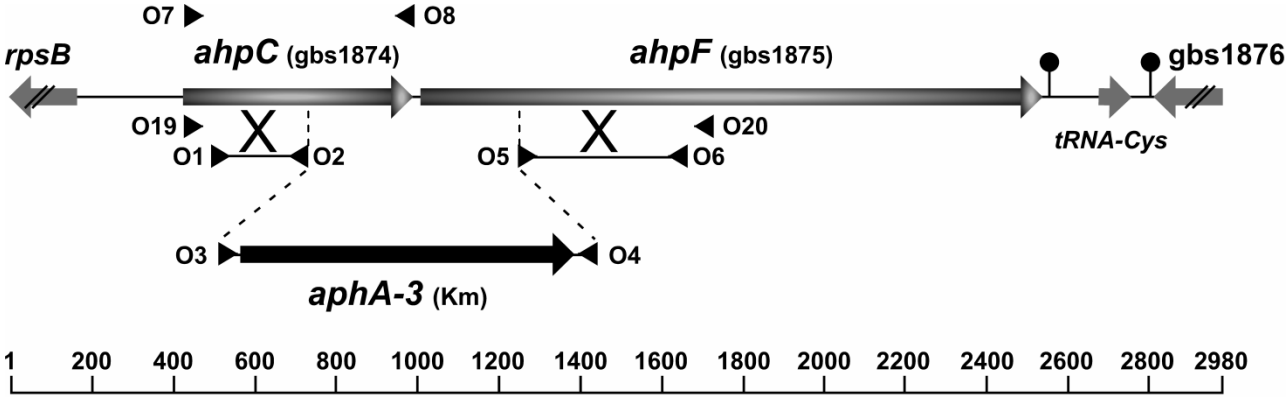

B

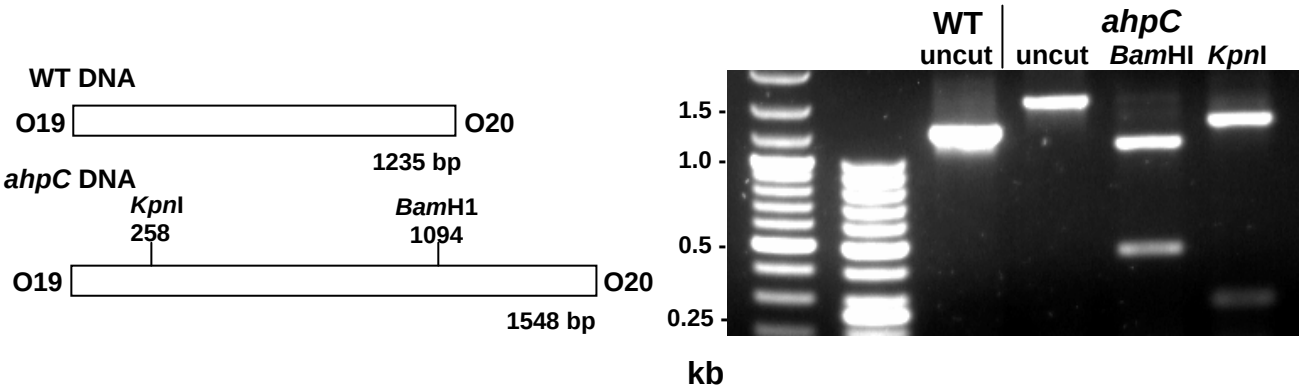

C

```
S.agalactiae NEM316      ....MSLVGK EIIEFSAQAY H.DGKFITVT NEDVKGKWAV FCFYPADFSF
L.lactis MG1363          ....MSLVGK KIEEFSTDAY L.GGKFIKVS DKDFYGKWSV LCFYPADFSF
Rattus norvegicus HBP23  MSSGNAKIGH PAPSFKATAV MPDGQFKDIS LSDYKGKYVV FFFYPLDFTF

S.agalactiae NEM316      VCPTELGDLQ EQYETLKSLD VEVYSVSTDT HFVHKAW... HDDSDVVGTI
L.lactis MG1363          VCPTELEDLE ETYPTLKSLG VEVYSASTDT HFVHAAW... HEHSDAISKI
Rattus norvegicus HBP23  VCPTEIIAFS DRAEEFKKLN CQVIGASVDS HFSHLAWINT PKKQGGLGPM

S.agalactiae NEM316      TYPMIGDPSH LISQGFDVLG QD.GLAQRGT FIIDPDGVIQ MMEINADGIG
L.lactis MG1363          TYPMLADPSQ KISRAFDVLD EEAGLAQRGT FIIDPDGVIQ ALEITADGIG
Rattus norvegicus HBP23  NIPLVSDPKR TIAQDYGVLK ADEGISFRGL FIIDDKGILR QITINDLPVG

S.agalactiae NEM316      RDASTLIDKV RAAQYIRQHP GEVCPAKWKE GAETLTPSLD LVGKI.....
L.lactis MG1363          RDASQLVDKI KAAQYVRNHP GEVCPAKWKE DGASLHVGID LVGKI.....
Rattus norvegicus HBP23  RSVDEILRLV QAFQFTDKH. GEVCPAGWKP GSDTIKPDVN KSKEYFSKQK
```

Supplementary Figure 1

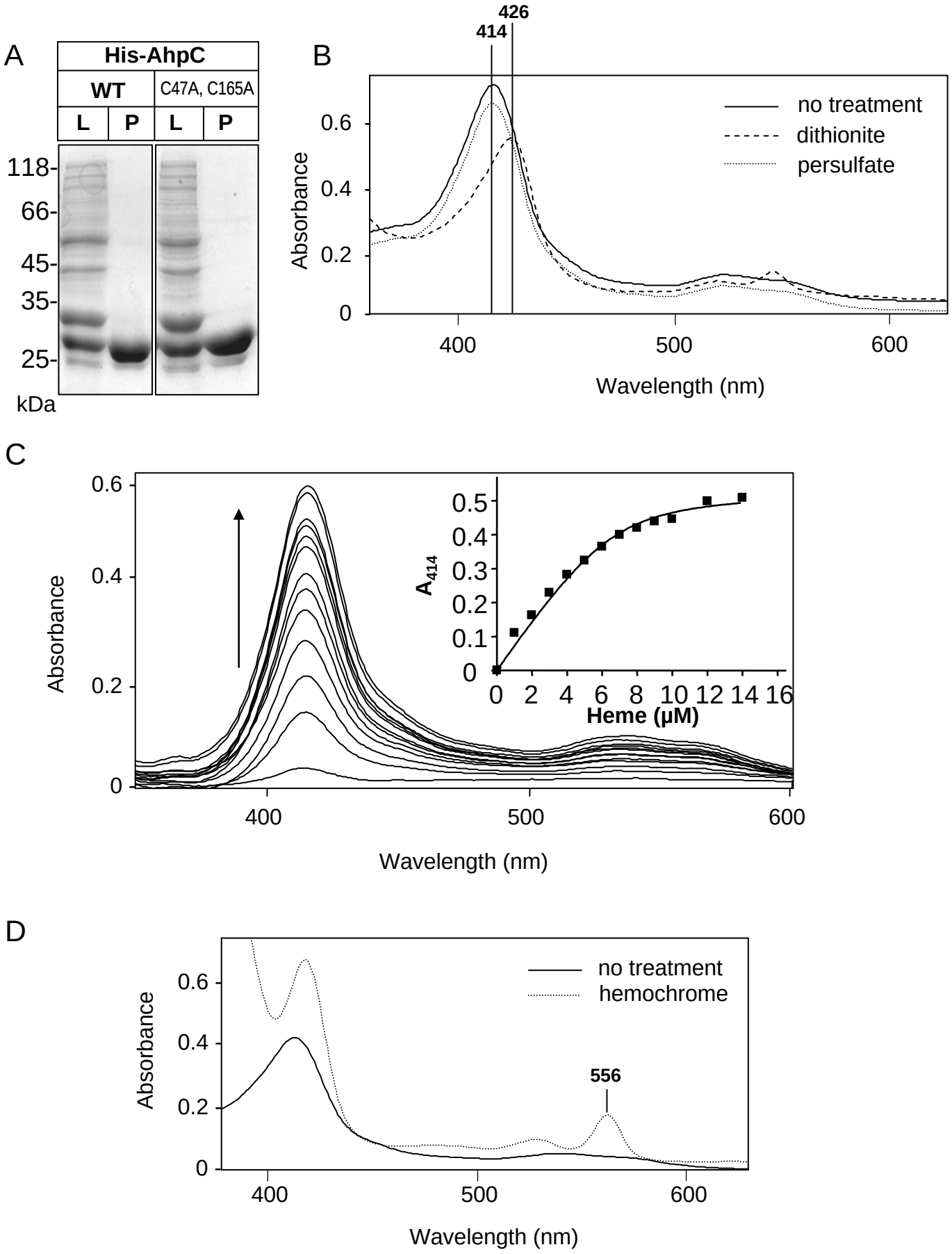

Supplementary Figure 2

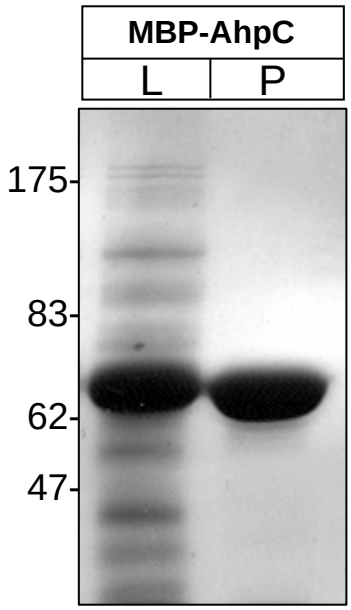

Supplementary Figure 3

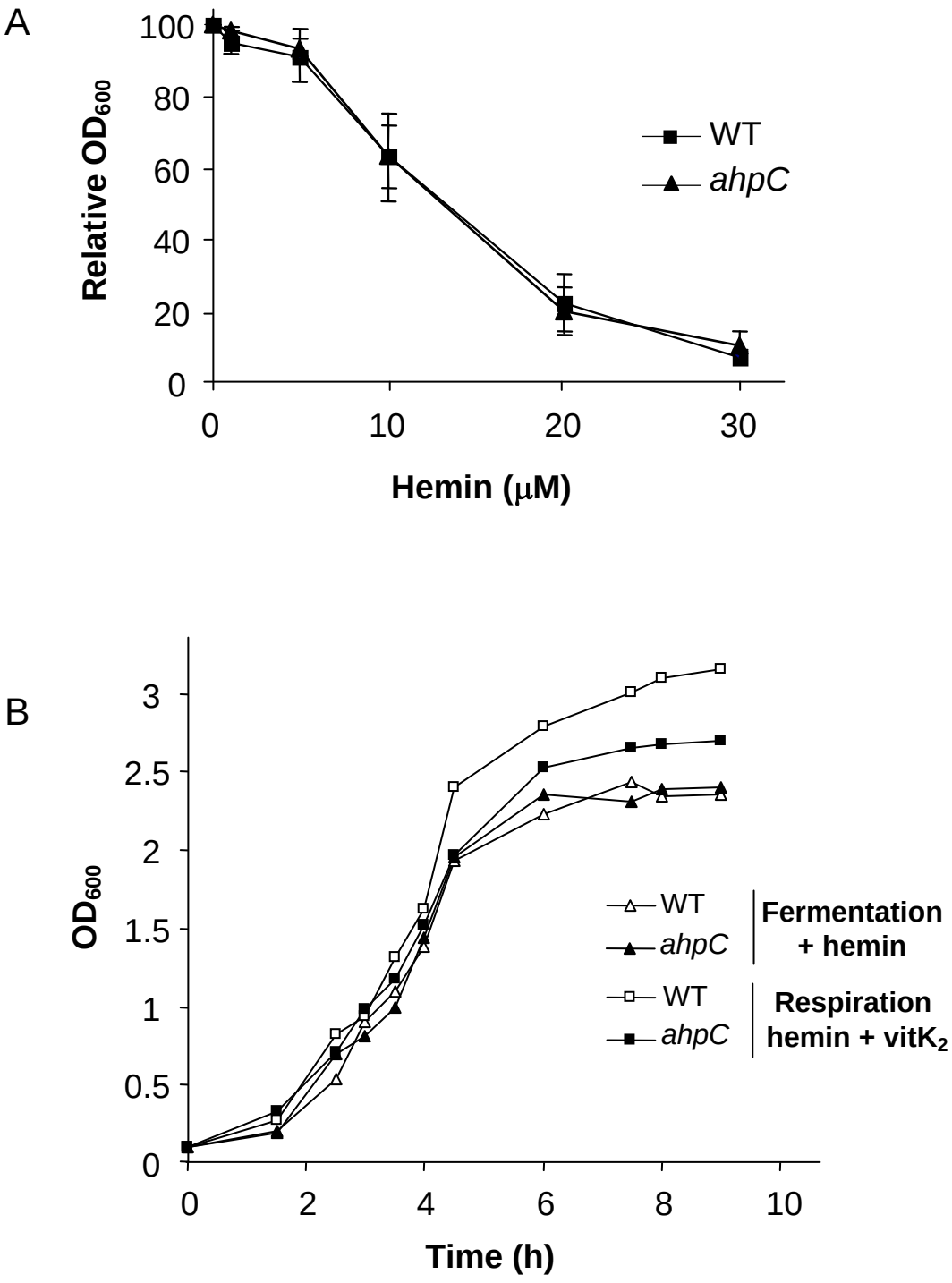

Supplementary Figure 4